

Universal Holonomic Quantum Gates in Decoherence-free Subspace on Superconducting Circuits

Zheng-Yuan Xue and Jian Zhou

*Guangdong Provincial Key Laboratory of Quantum Engineering and Quantum Materials,
and School of Physics and Telecommunication Engineering,
South China Normal University, Guangzhou 510006, China*

(Dated: November 18, 2018)

To implement a universal set of quantum logic gates based on non-Abelian geometric phases, one needs quantum systems that are beyond two levels. However, this is extremely difficult for superconducting qubits, and thus the recent experiment has only realized single qubit gates [A. A. Abdumalikov Jr et al., *Nature* 496, 482 (2013)]. Here, we propose to implement non-adiabatic holonomic quantum computation in decoherence-free subspace on circuit QED, where we only use two levels in transmon qubits, and require minimal resources for the decoherence-free subspace encoding. In this way, our scheme avoids difficulties in previous works while still can achieve considerable large effective coupling strength and thus leads to high fidelity quantum gates. Therefore, our scheme presents a promising way for robust quantum computation on superconducting circuits.

PACS numbers: 03.67.Lx, 42.50.Dv, 85.25.Cp

Under adiabatic cyclical evolution, a quantum system acquires a phase factor, which has both dynamical and geometric components. When the eigenstates of the system is non-degenerate, the geometric component is the famous Berry phase [1]. For the degenerate case, it is found to be a unitary operator acting on the degenerate subspace, i.e., holonomy [2]. As geometric phases are determined by the global property of the evolution path, the geometric way of quantum computation has shown to possess some built-in noise-resilience features [3–10]. In general, the holonomies are not commute with each other, and thus can be used to construct universal set of quantum gates [11–22], i.e., the holonomic quantum computation (HQC).

However, the adiabatic way of quantum computation intrinsically leads to slow gate speed, which may comparable with the lifetime of typical qubits [23, 24]. This motivates the research on the preferable non-adiabatic geometric phases. Recently, non-adiabatic HQC has been proposed with three-level lambda systems [25] with experimental demonstrations of elementary gates [26–29]. However, the upper excited state is resonantly coupled during the quantum evolution [25], and thus its limited lifetime is the main challenge in practical experiments. Note that this limitation may be avoided in experiments of Refs. [28] and [29] as they use the three magnetic states of a nitrogen-vacancy centre in a diamond. But, for superconducting transmon qubit, this limitation does exist and recent experiment only verified the single-qubit case [27]. The energy levels of a transmon qubit [30] form a ladder shape. The relatively small anharmonicity of the energy spectrum limits the coupling strength between neighbour levels to the order of 10 MHz in order to individually address the interactions [27, 31]. Therefore, even with newly demonstrated good coherent times of multi-levels in the transmon qubit [31], the implementation of

a nontrivial two-qubit, which needs much more complicated cavity induced interaction between two three-level systems[25], is still very challenging. Alternatively, there are schemes using much more complicated circuits than transmon to mimic multi-level systems [7, 16, 20]. However, this will inevitably introduce more noise effects from the environments due to the fact that more circuit and control elements are needed.

Meanwhile, there are many efforts to combine HQC with the decoherence-free subspace (DFS) encoding [32–34]. HQC in DFS [35–38] can consolidate both the noise-resilience of the encoding and the operational robustness of holonomies. As for transmon qubit, this will be much more difficult as this requires at least two transmon qubits to encode a logical qubit, and thus more complex interaction among qubits are needed, even in the single-qubit gate case. Previous proposed schemes considering HQC in DFS [35–38] usually need no less than three physical qubits to encode a logical qubit. However, it is well known that using two physical qubits is the minimum resource needed, as in Ref. [39] for geometric entangling gates.

Here, we propose to implement non-adiabatic HQC in DFS with typical circuit QED setup. Our scheme avoids the above mentioned difficulties. First, we only involve the two energy levels of a transmon qubit. Second, for the single-qubit case, our implementation based solely on effective resonate qubit-cavity interaction. Meanwhile, for the two qubit case, we only include the conventional detuned interaction, where the detuning between a transmon qubit and the cavity is fixed, and thus we may have plenty freedom to avoid the anharmonicity limitation. Third, we use two transmon to encode a logical qubit, which is minimal resource for the DFS encoding. Therefore, our scheme presents a promising way for HQC with superconducting circuits.

The setup we consider consists of driven transmon qubits couple to a transmission line resonator (1D cavity) [40]. A transmon qubit consists of two identical Josephson junction in a loop configuration and shunted by a large capacitance. The transmon qubit is quantized and its lowest two energy levels can be used to construct our physical qubit states with effective Hamiltonian $H_{q,j} = \omega_{q,j} \sigma_j^z / 2$, where we have assumed that $\hbar = 1$, $\omega_{q,j}$ is the energy splitting of the transmon qubit and σ_j^z is the Pauli matrix of the transmon qubit, which we labeled j , in its eigenbasis. For typical experimental values, $\omega_{q,j} \sim [4, 10]$ GHz [41]. The transmon qubits are located at the voltage antinodes of the relevant cavity mode, $H_c = \omega_c a^\dagger a$ with ω_c , a and a^\dagger are the frequency, annihilation and creation operators of the cavity, respectively. The coupled system is described by [41]

$$H_{JC} = H_c + \sum_{j=1}^n \left[H_{q,j} + g(\sigma_j a^\dagger + \sigma_j^\dagger a) \right], \quad (1)$$

where g , assuming to be real, is the qubit-cavity coupling strength, σ_j is the transmon lower operator and $\sigma_j^\dagger = (\sigma_j)^\dagger$. Here, we consider the case of $\Delta = (\omega_q - \omega_c) \gg g$ i.e., the qubit-photon interaction acts perturbatively. To get resonate interact between a selected transmon qubit with the cavity, the qubit is biased by an ac magnetic flux, which will introduce periodical modulation of the qubit transition frequency in the form of [40]

$$\omega_{q,j}(t) = \omega_q + \frac{\varepsilon_j}{2} \sin(\omega_j t + \varphi_j). \quad (2)$$

This modulation may effectively turn the qubit's sideband on resonance with the cavity frequency. To explicitly show this, we move to the rotating frame defined by

$$U(t) = \exp \left\{ -i \sigma_j^z \left[\omega_q t - \frac{\varepsilon_j}{2 \omega_j} \cos(\omega_j t + \varphi_j) \right] - i \omega_c a^\dagger a \right\},$$

when $\omega_j = \Delta$, we obtain the effective resonate qubit-cavity interaction as

$$H_d = g_j \sigma_j a^\dagger + \text{H.c.}, \quad (3)$$

where $g_j = g J_1(\alpha_j) \exp(i\varphi_j)$ with $\alpha_j = \varepsilon_j / \omega_j$, $J_m(z)$ are Bessel functions of the first kind and we have absorb a constant phase factor of $\pi/2$ into φ_j . In this way, we can obtain fully control over the coupling strength g_j from the external driven ac magnetic flux, i.e., by controlling the amplitude ε_j and phase φ_j . Note that the resonate interaction in Eq. (3), for more than two qubits case, has the conserved quantity of total excitation $N = \sum_{j=1}^n \sigma_j^\dagger \sigma_j + n_c$ with n_c being the photon number in the cavity.

Now, we proceed to deal with the holonomies for single qubit gates in DFS. Hereafter, to avoid confusing, we call our physical transmon qubits as transmons and logical qubits as qubits for short. As the transmons are placed in a same cavity, they are treated as interacting with the

same cavity induced dephasing environment. The DFS we consider here is the subspace of

$$S_1 = \{|100\rangle, |010\rangle, |001\rangle\} \equiv \{|0\rangle_L, |1\rangle_L, |E\rangle_L\}, \quad (4)$$

where the subscript L denote the states belong to the logical qubit and $|100\rangle \equiv |1\rangle_1 \otimes |0\rangle_2 \otimes |0\rangle_c$, i.e., they denote the states of the first and second transmons, and the cavity, respectively. In this way, we also use the cavity as an ancillary, and thus only two transmons are needed to encode a logical qubit. Note that the DFS is identical to the $N = 1$ subspace, which assures that the quantum dynamics will not go out the subspace S_1 .

In this encoding, the Hamiltonian of the quantum system consists of two transmons, i.e., $j \in \{1, 2\}$, resonate couple to a cavity reduces to

$$\begin{aligned} H_1 &= g_1 |E\rangle_L \langle 0| + g_2 |E\rangle_L \langle 1| + \text{H.c.} \\ &= \xi_1 \left(\sin \frac{\theta}{2} e^{i\varphi} |E\rangle_L \langle 0| - \cos \frac{\theta}{2} |E\rangle_L \langle 1| + \text{H.c.} \right) \end{aligned} \quad (5)$$

where $\xi_1 = g \sqrt{J_1(\alpha_1)^2 + J_1(\alpha_2)^2}$ is the effective Rabi frequency, $\tan(\theta/2) = J_1(\alpha_1)/J_1(\alpha_2)$, and $\varphi = \varphi_1 - \varphi_2 - \pi/2$. In this way, we construct a lambda type Hamiltonian in the DFS with only resonate transmon-cavity interaction, from which arbitrary single qubit holonomic gate can be induced.

In the dress state representation, the Hamiltonian in Eq. (5) can be viewed as that the state $|2\rangle_L$ only couples with the "bright" state $|b\rangle = \sin \frac{\theta}{2} e^{-i\varphi} |0\rangle - \cos \frac{\theta}{2} |1\rangle$, while decouples from the "dark" state $|d\rangle = \cos \frac{\theta}{2} |0\rangle + \sin \frac{\theta}{2} e^{i\varphi} |1\rangle$. Therefore, its evolution operator $U(t) = \exp(-i \int_0^t H_1 dt')$ reduces to holonomic gates if the following two conditions are satisfied [25]. First, the duration of the Hamiltonian must chosen to meet $\int_0^{\tau_1} \xi_1 dt = \pi$, which ensures the cyclic evolution condition. Second, $\langle \psi_i(t) | H_1 | \psi_j(t) \rangle = 0$ with $|\psi_{i,j}(t)\rangle$ being the time dependent qubit states, which ensures the evolution is pure geometric and the parallel-transport condition will be satisfied at any time due to the structure of the Hamiltonian other than the slow evolution. Under these two conditions, in the logical qubit subspace $\{|0\rangle_L, |1\rangle_L\}$, the non-adiabatic holonomic gates can be realized as

$$U(\theta, \varphi) = \begin{pmatrix} \cos \theta & \sin \theta e^{-i\varphi} \\ \sin \theta e^{i\varphi} & -\cos \theta \end{pmatrix} \quad (6)$$

where θ and φ can be tuned by choosing approximate parameters of the external driven ac magnetic fluxes. Therefore, arbitrary single-qubit gate can be obtained.

The performance of this gate can be evaluated by considering the influence of dissipation using the quantum master equation of

$$\begin{aligned} \dot{\rho} &= i[\rho, H_1 + H'_1] + \frac{\kappa}{2} \mathcal{L}(a) \\ &\quad + \frac{\Gamma_1}{2} \mathcal{L}(\sigma_1 + \sigma_2) + \frac{\Gamma_2}{2} \mathcal{L}(\sigma_1^z + \sigma_2^z), \end{aligned} \quad (7)$$

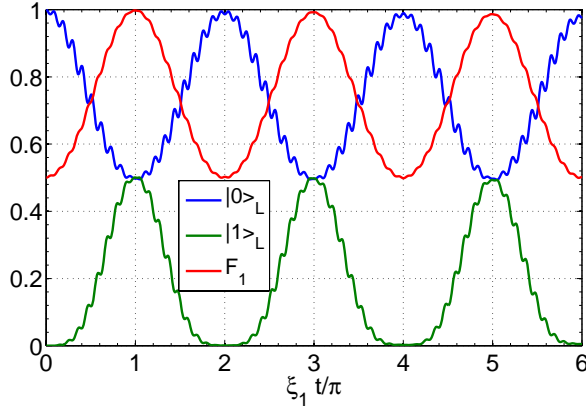


FIG. 1. (Color online) Qubit states population and fidelity dynamics of the Hadamard gate as a function of $\xi_1 t / \pi$.

where ρ is the density matrix of the considered system, $\mathcal{L}(A) = 2A\rho A^\dagger - A^\dagger A\rho - \rho A^\dagger A$ is the Lindblad operator, κ , Γ_1 and Γ_2 are the decay rate of the cavity, the decay and dephasing rates of the qubits, respectively. We have assumed that the decay and the dephasing of the two transmons are the same. In writing the Hamiltonian in Eq. (3), we have applied the rotating wave approximation by neglecting the oscillating terms and the smallest oscillating frequency is Δ , i.e.,

$$H'_1 = g\sigma_j a^\dagger \left[J_0(\alpha_j)e^{-i\Delta t} + J_2(\alpha_j)e^{i(\Delta t + \varphi_j)} \right] + \text{H.c.} \quad (8)$$

We consider the Hadamard gate as a typical example, where $\theta = \pi/4$ and $\varphi = 0$. To make the total coupling to be strong, we may choose $J_1(\alpha_1) \simeq 0.21$ and $J_1(\alpha_2) \simeq 0.5$, which corresponds to $J_1(\alpha_1)/J_1(\alpha_2) = 0.42 \simeq \tan(\theta/2)$. This can be achieved by modulating $\alpha_1 = \varepsilon_1/\Delta \simeq 0.43$ and $\alpha_2 = \varepsilon_2/\Delta \simeq 1.21$, the tuning of coupling strength in this way has been experimentally demonstrated [40]. We may choose $\Delta = 2\pi \times 500$ MHz and $g = 2\pi \times 50$ MHz. As we only involved two levels in a transmon, we may set that the cavity frequency is the large one, and thus avoid the cross talk to other higher levels. Therefore, $\xi_1 \simeq 0.54g = 2\pi \times 27$ MHz. As $J_0(\alpha_1)/J_2(\alpha_1) > 40$, the $J_2(\alpha_1)$ term can be safely neglected for transmon 1. Meanwhile, for transmon 2, this ratio is also larger than 4. Therefore, in our numerical simulation, for demonstration purpose, we only include the J_0 terms in Eq. (8) for the two transmons. For a cavity with $\omega_r \simeq 2\pi \times 8$ GHz, the decay rate is $\kappa \simeq 2\pi \times 7$ kHz [42]. For a planar transmon, its relaxation and coherence times of 44 and 20 μs are reported [43], which corresponds to $\Gamma_1 \simeq 2\pi \times 8$ kHz and $\Gamma_2 \simeq 2\pi \times 3.5$ kHz. As κ , Γ_1 and Γ_2 are all on the same order, for simplicity, we treat them to be identical and set as $\Gamma_1 = \Gamma_2 = \kappa = 2\pi \times 10$ kHz. Suppose the qubit is initially in the state of $|0\rangle_L$, we evaluate this gate by the qubit states population and the fidelity defined by $F_1 = \langle \psi_f | \rho | \psi_f \rangle$ with $|\psi_f\rangle = (|0\rangle + |1\rangle)_L / \sqrt{2}$ being the

ideally final state under the Hadamard gate. As shown in Fig. 1, we obtain a very high fidelity $F_1 \simeq 99.8\%$ at $t = \pi/\xi_1 \simeq 18.5$ ns.

Next, we turn to the implementation of a nontrivial two-qubit gate. In this case, we consider there are four transmons in the cavity, and there exists a six-dimensional DFS

$$\begin{aligned} S_2 = \{ & |00\rangle_L = |10100\rangle, |01\rangle_L = |10010\rangle, \\ & |10\rangle_L = |01100\rangle, |11\rangle_L = |01010\rangle, \\ & |a_1\rangle = |11000\rangle, |a_2\rangle = |00110\rangle \}, \end{aligned} \quad (9)$$

where $|10100\rangle \equiv |1\rangle_1|0\rangle_2|1\rangle_3|0\rangle_4|0\rangle_c$; $|a_1\rangle$ and $|a_2\rangle$ are two ancillary states, both of which have two excitations within a logical qubit and thus will not be affected in the single-qubit cases (in the $N = 1$ subspace).

To obtain a nontrivial two-qubit gate, we need to induce the interaction between two transmon pairs, i.e., transmons 2 and 3, 2 and 4, while avoid interaction between other pairs. To achieve this, for transmons 3 and 4, we do not apply external driven and set $\delta = (\omega_{q,4} - \omega_c) = (\omega_c - \omega_{q,3}) = 2\pi \times 300$ MHz. While transmon 2 we modulate the frequency of the external driven ac magnetic flux to be $\omega'_2 = 2\delta$. In this way, we may implement large detuning interaction and in the mean time avoid the anharmonicity limitation.

In the rotating frame, the interaction Hamiltonian for the transmon-cavity system is

$$\begin{aligned} H_{\text{int}} = & ga^\dagger \sigma_2 \left[J_0(\beta)e^{-i\delta t} + J_1(\beta)e^{i(\delta t + \varphi'_2 - \pi/2)} \right] \\ & + ga^\dagger \sigma_3 e^{i\delta t} + ga^\dagger \sigma_4 e^{-i\delta t} + \text{H.c.}, \end{aligned} \quad (10)$$

where $\beta = \varepsilon'_2/\omega'_2$. When $\delta \gg g$, the effective Hamiltonian for this interaction is

$$H_{\text{eff}} = \frac{g^2}{\delta} \left[J_0(\beta)\sigma_2\sigma_4^\dagger - J_1(\beta)e^{i\phi}\sigma_2\sigma_3^\dagger \right] + \text{H.c.}, \quad (11)$$

where $\phi = \varphi'_2 - \pi/2$ and we have neglected the stark shift terms. In the subspace S_2 , the above effective Hamiltonian reads

$$\begin{aligned} H_2 = & -\xi_2 \left[\sin \frac{\vartheta}{2} e^{i\phi} (|a_1\rangle_L \langle 00| + |11\rangle_L \langle a_2|) \right. \\ & \left. - \cos \frac{\vartheta}{2} (|a_1\rangle_L \langle 01| + |10\rangle_L \langle a_2|) + \text{H.c.} \right] \end{aligned} \quad (12)$$

where $\tan(\vartheta/2) = J_1(\beta)/J_0(\beta)$ and the effective Rabi frequency $\xi_2 = (g^2/\delta)\sqrt{J_0(\beta)^2 + J_1(\beta)^2}$. The effective Hamiltonian in Eq. (12) can be rewrite into two commute parts as $H_2 = H_a + H_b$ with

$$\begin{aligned} H_a = & -\xi_2 \left[\sin \frac{\vartheta}{2} e^{i\phi} |a_1\rangle_L \langle 00| - \cos \frac{\vartheta}{2} |a_1\rangle_L \langle 01| \right] + \text{H.c.}, \\ H_b = & -\xi_2 \left[\sin \frac{\vartheta}{2} e^{-i\phi} |a_2\rangle_c \langle 11| - \cos \frac{\vartheta}{2} |a_2\rangle_c \langle 10| \right] + \text{H.c.} \end{aligned}$$

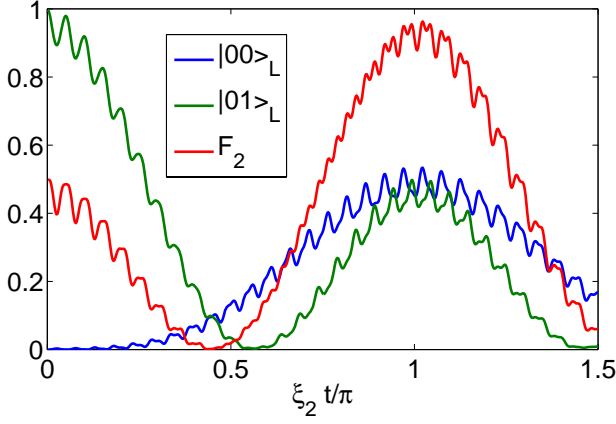


FIG. 2. (Color online) Qubit states population and fidelity dynamics of the $U(\pi/4, 0)$ gate as a function of $\xi_2 t/\pi$.

When $\xi_2 \tau_2 = \pi$, the evolution operator in our logical qubit subspace reduces to

$$U(\vartheta, \phi) = \begin{pmatrix} \cos \vartheta & \sin \vartheta e^{-i\phi} & 0 & 0 \\ \sin \vartheta e^{i\phi} & -\cos \vartheta & 0 & 0 \\ 0 & 0 & -\cos \vartheta & \sin \vartheta e^{-i\phi} \\ 0 & 0 & \sin \vartheta e^{i\phi} & \cos \vartheta \end{pmatrix}. \quad (13)$$

We can see that the gate in the subspace $\{|00\rangle, |01\rangle\}$ is different from the one in the subspace $\{|10\rangle, |11\rangle\}$. Therefore, in general, this is a nontrivial two-qubit gate.

For example, when $\vartheta = \pi/4$ and $\phi = 0$, it reduces to

$$U\left(\frac{\pi}{4}, 0\right) = \frac{1}{\sqrt{2}} \begin{pmatrix} 1 & 1 & 0 & 0 \\ 1 & -1 & 0 & 0 \\ 0 & 0 & -1 & 1 \\ 0 & 0 & 1 & 1 \end{pmatrix}. \quad (14)$$

In this case $J_1(\beta)/J_0(\beta) = \tan(\pi/8)$, which leads to $\beta \simeq 0.77$, $J_0(\beta) = 0.86$, $J_1(\beta) = 0.36$, and thus $\xi_2 \simeq 7.7$ MHz. In addition, $J_1(0.77)/J_2(0.77) > 5$ and $J_2(0.77) \gg J_n(0.77)$ for $n > 2$. Moreover, the smallest oscillating frequency is 3Δ when $n = 2$, and thus the coupling between two transmons induced by the $J_2(0.77)$ term is smaller than 1% in strength compare with that of induced by the $J_1(0.77)$ term. Therefore, the higher order terms is neglected in Eq. (10). For the initial state $|01\rangle$, we simulated the performance of this gate using Hamiltonian in Eq. (10), as shown in Fig. 2, where we obtain a high fidelity of $F_2 \simeq 96.3\%$ at $t = \pi/\xi_2 \simeq 130$ ns.

In conclusion, we propose to implement HQC in DFS with typical circuit QED, where we only use two levels from conventional transmon qubits and minimal resources for decoherence-free subspace encoding. Our Scheme avoid difficulties in previous implementation of HQC with superconducting qubits and still can obtain considerable large effective interaction strength and thus leads to high fidelity quantum gates. Therefore, our

scheme presents a promising way of on-chip solid-state robust quantum computation.

This work was supported by the NFRPC (No. 2013CB921804) and the PCSIRT (No. IRT1243).

-
- [1] M. V. Berry, Proc. R. Soc. Lond. A **392**, 45 (1984).
 - [2] F. Wilczek, and A. Zee, Phys. Rev. Lett. **52**, 2111 (1984).
 - [3] G. Falci, R. Fazio, G. M. Palma, J. Siewert, and V. Vedral, Nature **407**, 355 (2000).
 - [4] D. Leibfried, B. DeMarco, V. Meyer, D. Lucas, M. Barrett, J. Britton, W. M. Itano, B. Jelenković, C. Langer, T. Rosenband, and D. J. Wineland, Nature **422**, 412 (2003).
 - [5] J. Du, P. Zou, and Z. D. Wang, Phys. Rev. A **74**, 020302(R) (2006).
 - [6] P. J. Leek, J. M. Fink, A. Blais, R. Bianchetti, M. Goppl, J. M. Gambetta, D. I. Schuster, L. Frunzio, R. J. Schoelkopf, and A. Wallraff, Science **318**, 1889 (2007).
 - [7] M. Möttönen, J. J. Vartiainen, and J. P. Pekola, Phys. Rev. Lett. **100**, 177201 (2008).
 - [8] M. Pechal, S. Berger, A.A. Abdumalikov, Jr., J. M. Fink, J. A. Mlynek, L. Steffen, A. Wallraff, and S. Filipp, Phys. Rev. Lett. **108**, 170401 (2012).
 - [9] S.-L. Zhu and P. Zanardi, Phys. Rev. A **72**, 020301(R) (2005).
 - [10] M. Johansson, E. Sjöqvist, L. M. Andersson, M. Ericsson, B. Hessmo, K. Singh, and D. M. Tong, Phys. Rev. A **86**, 062322 (2012).
 - [11] P. Zanardi and M. Rasetti, Phys. Lett. A **264**, 94 (1999).
 - [12] J. Pachos, P. Zanardi, and M. Rasetti, Phys. Rev. A **61**, 010305(R) (2000).
 - [13] J. A. Jones, V. Vedral, A. Ekert, and G. Castagnoli, Nature **403**, 869-871 (2000).
 - [14] L.-M. Duan, J. I. Cirac, and P. Zoller, Science **292**, 1695 (2001).
 - [15] A. Recati, T. Calarco, P. Zanardi, J. I. Cirac, and P. Zoller, Phys. Rev. A **66**, 032309 (2002).
 - [16] L. Faoro, J. Siewert, and R. Fazio, Phys. Rev. Lett. **90**, 028301 (2003).
 - [17] P. Zhang, Z. D. Wang, J. D. Sun, and C. P. Sun, Phys. Rev. A **71**, 042301 (2005).
 - [18] O. Oreshkov, T. A. Brun, and D. A. Lidar, Phys. Rev. Lett. **102**, 070502 (2009).
 - [19] V. N. Golovach, M. Borhani, and D. Loss, Phys. Rev. A **81**, 022315 (2010).
 - [20] I. Kamleitner, P. Solinas, C. Müller, A. Shnirman, and M. Möttönen, Phys. Rev. B **83**, 214518 (2011).
 - [21] N. Chancellor and S. Haas, Phys. Rev. A **87**, 042321 (2013).
 - [22] K. Toyoda, K. Uchida, A. Noguchi, S. Haze, and S. Urabe, Phys. Rev. A **87**, 052307 (2013).
 - [23] X.-B. Wang and M. Keiji, Phys. Rev. Lett. **87**, 097901 (2001).
 - [24] S. L. Zhu and Z. D. Wang, Phys. Rev. Lett. **89**, 097902 (2002).
 - [25] E. Sjöqvist, D. M. Tong, L. M. Andersson, B. Hessmo, M. Johansson, and K. Singh, New J. Phys. **14**, 103035 (2012).

- [26] G. Feng, G. Xu, and G. Long, *Phys. Rev. Lett.* **110**, 190501 (2013).
- [27] A. A. Abdumalikov Jr, J. M. Fink, K. Juliusson, M. Pechal, S. Berger, A. Wallraff, and S. Filipp, *Nature* **496**, 482 (2013).
- [28] C. Zu, W.-B. Wang, L. He, W.-G. Zhang, C.-Y. Dai, F. Wang, and L.-M. Duan, *Nature* **514**, 72 (2014).
- [29] S. Arroyo-Camejo, A. Lazarev, S. W. Hell, and G. Balasubramanian, *Nat. Commun.* **5**, 4870 (2014).
- [30] J. Koch, T. M. Yu, J. Gambetta, A. A. Houck, D. I. Schuster, J. Majer, A. Blais, M. H. Devoret, S. M. Girvin, and R. J. Schoelkopf, *Phys. Rev. A* **76**, 042319 (2007).
- [31] M. J. Peterer, S. J. Bader, X. Jin, F. Yan, A. Kamal, T. J. Gudmundsen, P. J. Leek, T. P. Orlando, W. D. Oliver, and S. Gustavsson, *Phys. Rev. Lett.* **114**, 010501 (2015).
- [32] L.-M. Duan, G.-C. Guo, *Phys. Rev. Lett.* **79**, 1953 (1997).
- [33] P. Zanardi, M. Rasetti, *Phys. Rev. Lett.* **79**, 3306 (1997).
- [34] D. A. Lidar, I. L. Chuang, K. B. Whaley, *Phys. Rev. Lett.* **81**, 2594 (1998).
- [35] L. A. Wu, P. Zanardi, and D. A. Lidar, *Phys. Rev. Lett.* **95**, 130501 (2005).
- [36] G. F. Xu, J. Zhang, D. M. Tong, E. Sjöqvist, and L. C. Kwek, *Phys. Rev. Lett.* **109**, 170501 (2012).
- [37] J. Zhang, L.-C. Kwek, E. Sjöqvist, D. M. Tong, and P. Zanardi, *Phys. Rev. A* **89**, 042302 (2014).
- [38] Z.-T. Liang, Y.-X. Du, W. Huang, Z.-Y. Xue, and H. Yan, *Phys. Rev. A* **89**, 062312 (2014).
- [39] X. L. Feng, C. F. Wu, H. Sun, and C. H. Oh, *Phys. Rev. Lett.* **103**, 200501 (2009).
- [40] J. D. Strand, M. Ware, F. Beaudoin, T. A. Ohki, B. R. Johnson, A. Blais, and B. L. T. Plourde, *Phys. Rev. B* **87**, 220505(R) (2013).
- [41] M. H. Devoret and R. J. Schoelkopf, *Science* **339**, 1169 (2013).
- [42] B. Vlastakis, G. Kirchmair, Z. Leghtas, S. E. Nigg, L. Frunzio, S. M. Girvin, M. Mirrahimi, M. H. Devoret, and R. J. Schoelkopf, *Science* **342**, 607 (2013).
- [43] R. Barends, J. Kelly, A. Megrant, D. Sank, E. Jeffrey, Y. Chen, Y. Yin, B. Chiaro, J. Mutus, C. Neill, P. O'Malley, P. Roushan, J. Wenner, T. C. White, A. N. Cleland, and J. M. Martinis, *Phys. Rev. Lett.* **111**, 080502 (2013).